

Power generation modeling for a wearable thermoelectric energy harvester with practical limitations



Kyle Pietrzyk, Joseph Soares, Brandon Ohara, Hohyun Lee*

Department of Mechanical Engineering, Santa Clara University, Santa Clara, CA 95053, United States

HIGHLIGHTS

- Explored the effect of practical issues in body heat thermoelectric energy harvester.
- Suggested optimal/practical geometries for the heat sink and thermoelectric module.
- Considered the effect of a boost converter's voltage dependent efficiency.
- Estimated power output of 0.48 mW within a wearable area.

ARTICLE INFO

Article history:

Received 21 June 2016

Received in revised form 27 August 2016

Accepted 29 August 2016

Keywords:

Boost converter
Practicality consideration
Module geometry
Heat sink optimization
Thermal load matching

ABSTRACT

Recent studies on improving the thermoelectric figure of merit (ZT) have advanced research into self-powered, wearable technologies using thermoelectric generators. However, previous design approaches do not consider structurally practical heat sink and module geometries, the use of a boost converter, or the size constraint of the generator due to aesthetic appeal, all of which lower the overall power output. Additionally, the reduced efficiency in using a boost converter changes the electrical and thermal load matching conditions for maximum power. In this study, the limitations of practicality were considered for a wearable thermoelectric generator that utilizes a state-of-the-art boost converter and an optimized heat sink. Heat sink fin geometries and thermoelectric module geometries were explored to maximize the power output within a 42.0 cm² area and a 1.0 cm total height, in order to justify the wearability of the energy harvester. With optimized values of fin and module heights, the system was designed to produce 0.48 mW of electrical power at a boosted output voltage of 3.0 V, enough to power a small heart-rate monitor.

© 2016 Elsevier Ltd. All rights reserved.

1. Introduction

Thermoelectric energy harvesters have the potential to free people from frequent charging and battery replacement of portable devices through their incorporation into wearable device applications. Thermoelectric generators convert waste heat from the human body into electrical energy without being interrupted via the Seebeck effect, which produces an electrical potential proportional to a temperature difference [1]. Unfortunately, the application of thermoelectric devices is often not practical or feasible due to their low voltage and power production, as well as their limited heat dissipation capability. The performance of thermoelectric devices depends on three material properties: thermal conductivity, the Seebeck coefficient, and electrical resistivity. Many

research efforts focus on improving these properties through nano-structuring or band gap engineering [2,3]. However, system level optimization has not yet been explored as extensively as the material properties and many practical issues have been overlooked.

Three main aspects have been ignored in designing an energy harvesting system with thermoelectric generators: limited heat dissipation from the cold side of the module, low system output voltage, and the limited practical size of the system. Another general practice in designing a thermoelectric power generator, which should be avoided, is the use of the traditional method for evaluating the maximum power generation, as it assumes an infinite amount of heat dissipation from the cold side. This implies that the cold side temperature is equal to the temperature of the ambient air around it [4,5], which leads to an overestimation of power production. In reality, a finite thermal resistance exists between the thermoelectric module and the ambient, causing the actual

* Corresponding author.

E-mail address: hlee@scu.edu (H. Lee).

temperature drop to be much larger than the value predicted by the traditional approach. Moreover, internal heat generation by Joule heating and the Peltier effect, which cause further change in temperature difference across thermoelectric materials, is often neglected in the load matching condition when utilizing the traditional approach [6]. In using energy conservation equations, the module's cold side thermal resistance and internal heat generations must be taken into account [7]:

$$Q_H = K(T_H - T_C) + SIT_H - \frac{1}{2}I^2R = \frac{T_{BODY} - T_H}{\psi_H} \quad (1)$$

$$Q_C = K(T_H - T_C) + SIT_C + \frac{1}{2}I^2R = \frac{T_C - T_\infty}{\psi_C} \quad (2)$$

where K is the thermal conductance of the module, T_H is the temperature of the module's hot side, T_C is the temperature of the module's cold side, S is the Seebeck coefficient of the module, I is the module's input current, R is the electrical resistivity of the module, T_{BODY} is the internal temperature of the human body, T_∞ is the ambient temperature, ψ_H is the thermal resistance of the wearer's skin, and ψ_C is the thermal resistance of the heat sink. Furthermore, K , S , and R may be described with the following equations:

$$S = N(\alpha_p - \alpha_n) \quad (3)$$

$$R = \frac{4N^2 \rho L + 8N^2 R_C}{A_S FF} \quad (4)$$

$$K = \frac{A_S k FF}{L} \quad (5)$$

where N is the number of leg pairs in the generator, α_p and α_n are the Seebeck coefficients of the p-type and n-type legs respectively, ρ is the electrical resistance of the thermoelectric material, L is the leg length, R_C is the electrical contact resistance between each leg, A_S is the surface area of the generator, k is the thermal conductivity of the thermoelectric material, and FF is the fill factor, which may be described with the following:

$$FF = \frac{2NA_C}{A_S} \quad (6)$$

where A_C is the cross-sectional area of a thermoelectric leg. With these equations, an appropriate model for a thermoelectric power generator can be created.

Recently, several researchers have realized the importance of thermal load matching to maximize the temperature difference across the module and increase the power and voltage output. Therefore, they have suggested a new power optimization strategy: matching the thermal resistances [8]:

$$\psi_{TEM} = (\psi_H + \psi_C) \sqrt{1 + ZT} \quad (7)$$

where ψ_{TEM} is the thermal resistance of the thermoelectric module and ZT is the dimensionless thermoelectric figure of merit, which is given by the following:

$$ZT = \frac{(\alpha_p - \alpha_n)^2 T}{k\rho} \quad (8)$$

where T is the temperature at which the figure of merit is being evaluated. Using this method, the maximum power can be produced when a thermoelectric power generator is designed to satisfy Eq. (7), assuming the electrical load matching condition is $R_L/R = \sqrt{1 + ZT}$, where R_L is the electrical load resistance and R is the module electrical resistance [1].

A more general approach to evaluate the power output for a thermoelectric generator is suggested by Youn et al. and McCarty and Piper [9,10]:

$$V_{OC} = S\Delta T_{OC} \quad (9)$$

$$V_{OUT} = \frac{V_{OC}}{2} \quad (10)$$

$$I_{SC} = S \frac{T_H - T_C}{R} \quad (11)$$

$$P_{MAX} = \frac{V_{OC} I_{SC}}{4} \quad (12)$$

where V_{OC} is the module's open circuit voltage, V_{OUT} is the output voltage of the module, I_{SC} is the short circuit current of the module, P_{MAX} is the maximum power output of the module for a given heat sink performance, and ΔT_{OC} is the open circuit temperature difference across the module. One should note that the temperature difference in Eq. (11) is different from that of Eq. (9) due to additional heat generation inside the module by Joule heating and the Peltier effect. Also, the power output is independent of the number of leg pairs, due to the assumption of negligible electrical contact resistance; however, the number of leg pairs will change the output voltage and current ranges of the system. While the temperature difference under the open circuit can be derived by a simple thermal circuit analogy, due to no internal heat generation by electrical current flow, the temperature difference under the short circuit should be calculated by solving Eqs. (1) and (2). In using Eqs. (9)–(12), it is assumed that the electrical load resistance ratio is such that the maximum power conditions are present [10], which differs from the traditional load matching condition. As demonstrated by Gomez et al. [7], when internal heat generation caused by Joule heating and the Peltier effect is taken into account, the maximum power output does not necessarily occur when the load resistance is matched with internal resistance [10]. However, Youn et al. has shown that the current and voltage curve of a thermoelectric power generator is straight, regardless of the thermal load being matched or not [9]. Therefore, the maximum power can be easily evaluated without numerically solving the energy conservation equations: the maximum power output happens when the voltage output is close to half the open circuit voltage (Eq. (10)) and the maximum power output is the product of the short circuit current and the open circuit voltage divided by four (Eq. (12)). However, these optimum conditions have two main limitations in wearable thermoelectric power generation design. Firstly, in order to maintain aesthetic appeal, wearable thermoelectric generators are limited in physical space, which makes it difficult to ensure thermal load matching. Secondly, the voltage output must be boosted to gain useful power out of the generator, which causes further reduction in the power output. Since the boost converter efficiency depends on its input voltage, the power output from a thermoelectric energy harvester is no longer independent of the voltage value. Therefore, the recent maximum power output conditions (Eqs. (7) and (12)) are no longer mathematically valid. For these reasons, new optimal module geometry and electrical load matching conditions must be suggested for the wearable energy harvester design.

In previous efforts, wearable thermoelectric generators have often been made far bulkier than desired and produce only a small amount of power. An earlier study shows that a thermoelectric device almost 3 cm tall could only produce 20–30 $\mu\text{W}/\text{cm}^2$ [11,12]. Suarez et al. used a 3D model to design and test a custom module, which was able to produce 120 μW [13]. More recently, a flexible thermoelectric generator with 100 leg pairs has been able to generate 4.18 nW and 160 mV with a temperature difference of 15 K across the module [14]. In investigating flexible thermoelectric generators, extensive research in organic semiconductor material for flexible thermoelectrics has been conducted by Chen et al. [15]. Such research can be used to enhance the output power of a thermoelectric power generation system by creating better contact

between the modules in the system and the user's skin. Also in the area of flexible thermoelectrics, Bahk et al. created a device that could produce 0.18 mW and 0.9 V by manipulating the thermoelectric material and gap filler material of the generator [16]. However, the effect of the module's output voltage on an implemented boost converter was not considered in this design or the calculations. Thermoelectric modules embedded in clothing have also been explored [12]; however, the power output is typically on the order of nanowatts and heat dissipation lacks due to limited space. This makes it incredibly difficult to harvest a significant amount of power from these thin filmed modules, as demonstrated by Min-Ki et al., who obtained 224 nW from a module area of 6×25 mm [17,18]. In order to obtain more power and voltage from such devices, thicker modules with improved heat dissipation devices are necessary, as they will allow a module to maintain a larger temperature difference. Longer thermoelectric legs will increase the temperature difference between the cold and hot sides of the module, while an improved heat dissipation system on the cold side of the module will help dissipate parasitic heat transfer from the applied body heat to the ambient. Both modifications will keep body heat from transferring to the cold side of the module and allow for a greater power output. Therefore, the thickness of the thermoelectric module and the heat dissipation device are taken into account in this study.

Previously explored designs provide unique methods for producing electrical power from body heat, but they do not fully address the issues with system integration. The issues (limited heat dissipation, low voltage output, and size limitation) of wearable thermoelectric power generators are linked to each other and must be addressed simultaneously. As such, this paper presents a framework for wearable energy harvest module design. Initially, the heat sink geometry for the cold side of the generator was optimized in order to lower the thermal resistance on the cold side of the module as much as possible. Practical and optimal module geometries for generating the maximum power were then explored with the consideration of the heat sink's thermal resistance. After, the effect of the produced voltage on the efficiency of a boost converter was analyzed and practical size constraints on the system were considered. Through these considerations, this work proposes a design of a wearable energy harvester with 480 μ W of power in a 42.0 cm² area around the user's wrist.

2. Modeling approach

Fig. 1 shows the schematics of a thermoelectric power generation system (Fig. 1a) and the module geometry (Fig. 1b). Since

the amount of voltage produced by a thermoelectric module is proportional to its temperature difference, it is crucial to determine the temperature difference across the module. This can be done by applying the previously presented energy conservation Eqs. (Eqs. (1) and (2)) at both ends of the generator. In doing this, it can be seen that in Eqs. (3)–(5), the leg length is always accompanied by $1/FF$. To simplify these equations, the B-factor, defined with the following equation, can be used.

$$B = \frac{L}{FF} \quad (13)$$

In using the B-factor, the number of module leg pairs can be eliminated from the energy conservation equations, while neglecting the electrical contact resistance in the module. This allows for easy manipulation of the module geometry when using the energy conservation equations. Also, as shown by Gomez et al., the input current in the energy conservation equations can be defined with the following equation [7]:

$$I = \frac{S(T_H - T_C)}{R(1+x)} \quad (14)$$

where x is the ratio between the electrical load resistance and the module electrical resistance. Substituting Eqs. (13) and (14) into Eqs. (1) and (2) yields the following equations:

$$Q_H = \frac{A_S k}{B} (T_H - T_C) + \frac{(\alpha_p - \alpha_n)^2 A_S (T_H - T_C)}{4B\rho(1+x)} T_H - \frac{A_S}{8B\rho} \left(\frac{(\alpha_p - \alpha_n)(T_H - T_C)}{(1+x)} \right)^2 = \frac{T_{BODY} - T_H}{\psi_H} \quad (15)$$

$$Q_C = \frac{A_S k}{B} (T_H - T_C) + \frac{(\alpha_p - \alpha_n)^2 A_S (T_H - T_C)}{4B\rho(1+x)} T_C + \frac{A_S}{8B\rho} \left(\frac{(\alpha_p - \alpha_n)(T_H - T_C)}{(1+x)} \right)^2 = \frac{T_C - T_\infty}{\psi_C} \quad (16)$$

By using the conservation of energy and equating Eqs. (15) and (16), the total amount of heat transferred by Joule heating, the Peltier effect, and heat conduction is found to be equal to the amount of heat transferred to the heat sink from the heat source. Hence, the power generation is a function of the material properties, module geometry, and heat dissipation capabilities (thermal resistance) at both sides of the module. In analyzing Eqs. (15) and (16), the thermal resistances between the thermoelectric module and the heat source and sink are seen to be major limiting factors to the power output of the system. Fortunately, the heat sink and module geometries can be altered to minimize the cold side thermal

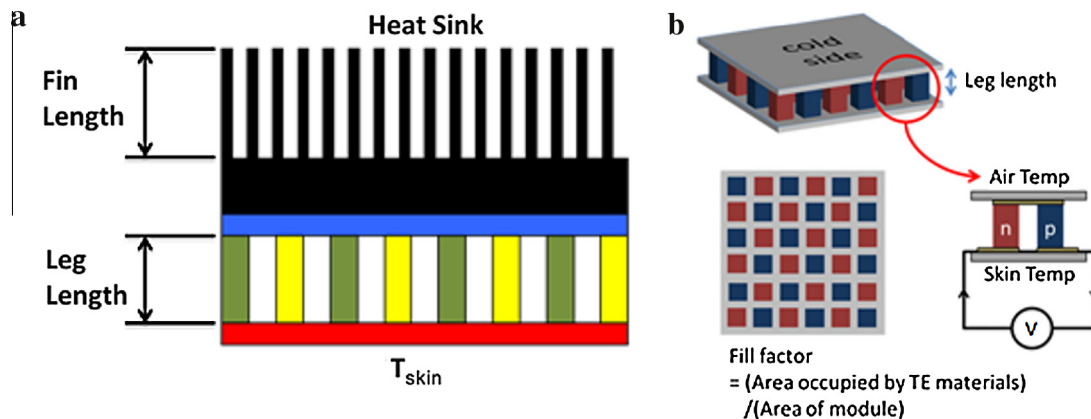


Fig. 1. (a) A schematic of the thermal system for a thermoelectric energy harvester, where body heat conducts through the thermoelectric module and the heat sink and (b) the considered geometric aspects of a thermoelectric module.

resistance and the module thermal resistance, respectively. Nusselt number correlations found in Bergmann et al. and Bejan [19,20] can be used to optimize the heat sink geometry, while the B-factor can be altered to optimize the module geometry. Since the hot side thermal resistance, ψ_H , is relatively fixed and can only be minimized by obtaining good contact between the user's skin and the module, it is determined using the 1D conduction resistance model displayed in Eq. (17).

$$\psi_H = \frac{t_{skin}}{k_{skin}A_{skin}} \quad (17)$$

where k_{skin} is the thermal conductivity of human skin, t_{skin} is the average thickness of human skin, and A_{skin} is the wrist area that will come into contact with the thermoelectric generator. In considering a wearable energy harvester, the thermal resistance on the cold side of the module is considered the limiting resistance, as forced convection is typically not an option. Therefore, the minimum allowable thermal resistance on the cold side of the module, where the heat is dissipated, must be investigated first. In this study, parallel rectangular fins made of aluminum are adopted for modeling.

As shown, Fig. 2a describes a generic parallel plate heat sink and the three geometric parameters (height, pitch, and gap between the fins) that are typically varied to minimize a heat sink's thermal resistance. For the application of wearable thermoelectric generators, the height is constrained to small lengths due to aesthetic reasons and the pitch can be found based on an optimized gap size and a desired number of fins. Since more surface area in a heat sink allows for greater convective heat transfer and a lower thermal resistance, it is desired that the surface area of the fins is maximized. To increase the surface area of the fins, the gap size can be decreased to allow for more fins in the heat sink. However, if the gap size is decreased too much, the thermal boundary layers of the fins will overlap in the gaps, reducing the convective heat transfer coefficient (h) and ultimately increasing the thermal resistance of the heat sink. This implies the existence of an optimum gap size, which will allow a heat sink to have a minimum thermal resistance. Additionally, as demonstrated in Fig. 2b, the overall

thickness of the boundary layer is dependent on the height of the fins, creating a relationship between the height and ideal gap size.

In order to evaluate the thermal resistance of a parallel plate heat sink, Eq. (18), which assumes an adiabatic fin tip boundary condition, is used [19,20].

$$\psi_C = \left[n \sqrt{hpk_{sink}A_{fin} \tanh(mH)} \right]^{-1} \quad (18)$$

where n is the number of fins in the heat sink, h is the convective heat transfer coefficient, p is the perimeter a single heat sink fin, k_{sink} is the thermal conductivity of the heat sink material (aluminum), A_{fin} is the cross-sectional area of a single fin, H is the fin height, and m is determined with the following equation:

$$m = \sqrt{\frac{hp}{k_{sink}A_{fin}}} \quad (19)$$

To find the convective heat transfer coefficient, the Nusselt number correlation for natural convective channel flow, as displayed in Eq. (20), can be used [19,20].

$$\overline{Nu}_D = \frac{DRa_D}{24H} \left[1 - \exp\left(-\frac{35H}{Ra_D D}\right) \right]^{\frac{3}{4}} = \frac{hD}{k_{air}} \quad (20)$$

where D is gap width of the heat sink, k_{air} is the thermal conductivity of the fluid (air), and Ra_D is the Rayleigh number. In using Eq. (18) to find the thermal resistance of the heat sink, the heat transfer from the fin tips and the base portion of the heat sink is not taken into account. This creates an overestimate in the thermal resistance of the heat sink, causing the results from this analysis to be conservative.

Using the provided Nusselt number equation to calculate the natural convective heat transfer coefficient on a parallel plate heat sink assumes the heat sink is right-side up. However, since the thermoelectric power generator being analyzed is planned to wrap around a person's wrist, it is inevitable that part of the heat sink will be upside-down. In seeing this dilemma, the following equations can be used to find the Nusselt number, and ultimately the

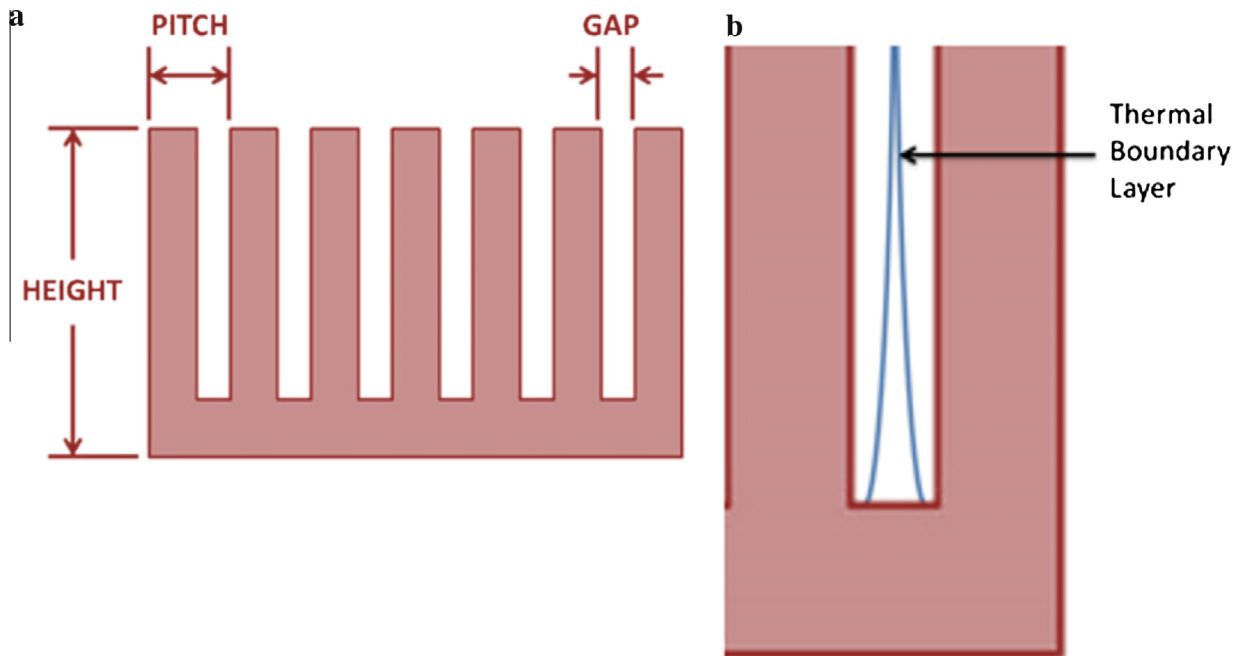


Fig. 2. (a) The height, pitch, and gap of the heat sink were varied to minimize the thermal resistance of the thermoelectric generator system's cold side and (b) the thermal boundary layer is shown in an enlarged view of a channel from the parallel fin heat sink.

convective heat transfer coefficient, for a heat sink experiencing natural convection upside-down [21].

$$\overline{Nu}_l = \frac{\overline{Nu}_l^S}{1 + \frac{2H}{D}} \left[\exp\left(-\frac{H}{D}\right) + 0.65 \left(\frac{2H}{D}\right) \left(\frac{2l}{D}\right)^{-\frac{4}{3}} Ra_l^{\frac{1}{4}} \right] \quad (21)$$

where l is the array half-length, Ra_l is the Rayleigh number, and \overline{Nu}_l^S is the average Nusselt number for a horizontal, infinite flat plate, which may be calculated using Eq. (22) [21]:

$$\overline{Nu}_l^S = [1 + 0.24 \exp(-0.0025l^*)] 0.46 Ra_l^{\frac{1}{4}} \quad (22)$$

where l^* may be described with the following equation [21]:

$$l^* = \frac{l}{\sqrt[3]{k\nu/g}} \quad (23)$$

Since the heat sink on the thermoelectric power generator is not entirely right-side up or upside-down due to the curvature of a person's wrist, finding the different convective heat transfer coefficients with the Nusselt number equations for both cases allows for the calculation of a range of heat sink thermal resistance values.

In order to utilize the heat sink related correlations and evaluate the thermal resistance of the heat sink in this study, geometric parameters of the heat sink were varied. By altering the gap size and fin thickness, the number of fins was determined assuming a fixed heat sink area. The fin thickness was then multiplied by the fin depth to calculate the cross-sectional area of each fin. The perimeter of a single fin was also calculated by multiplying the sum of the thickness and depth by two. The fin height was also varied in this analysis; however, its range was limited, as tall fins would decrease the aesthetic appeal of the thermoelectric device. Using these parameters, the necessary material properties, and the stated equations, the thermal resistance of the heat sink was calculated. Furthermore, the thermal resistance of the heat sink was assumed to be one dimensional, as the small ratio of fin length to depth of the system made heat transfer in any other direction but the vertical direction negligible. The spreading resistance of the heat sink's base was also assumed to be negligible, since the thermoelectric generator equally distributed heat across its face through alumina contact pads.

After minimizing the heat sink's thermal resistance, the module geometry was optimized to fully utilize the benefits of the low cold side thermal resistance. Using Eqs. (15) and (16), the B-factor was varied to find the optimal design of the thermoelectric module that would provide the greatest amount of power with the optimized heat sink. By solving Eqs. (15) and (16), the temperatures on the hot and cold sides of the module could be found and, ultimately, the output voltage and power of the thermoelectric generator could be calculated using the following equations [7]:

$$V = \frac{(S(T_H - T_C))x}{(x + 1)} \quad (24)$$

$$P = IV = \frac{(S(T_H - T_C))^2 x}{R(x + 1)^2} \quad (25)$$

It is important to note that the equations used for analyzing the outputs of the thermoelectric generator (Eqs. (24) and (25)) are different than Eqs. (9)–(12). The reason for this is a state-of-the-art micro-power boost converter (TI BQ25504) was incorporated into the system to boost the wearable thermoelectric generator's low voltage output to an appropriate level for electronic devices (3.0V). In using a boost converter, the effects of the boost converter's efficiency on the system needed to be considered, as the efficiency was highly dependent on the input voltage from the thermoelectric module.

The efficiency of the boost converter is presented in Fig. 3. Additionally, the final power output with consideration of the boost converter was determined with Eq. (26):

$$P_{OUT} = P\varepsilon(V) \quad (26)$$

where ε is the efficiency of the boost converter at a specific module output voltage, V .

As seen in Fig. 3, it is important for the module to maintain a high enough voltage for the boost converter to have a high overall power output from the system.

The last challenge of the modeling approach was keeping the total height of the entire system, including the fin height and thickness of the thermoelectric module, within a wearable and aesthetically pleasing constraint. Taller fin heights are typically desired for a smaller thermal resistance; however, having a tall fin height in the application of wearable thermoelectrics reduces the amount of thickness available for the thermoelectric module. As previously stated, utilizing a thin thermoelectric module makes it more difficult to maintain a large temperature difference across the module, resulting in a low power output. However, having longer thermoelectric legs limits the heat sink's fin height, which also reduces the power output. Hence, an optimum combination of the module leg length and the fin height must exist. Calculations were completed for a range of practical fin heights and module leg lengths. In these calculations, the fin height and module leg length were varied separately from 1.0 mm to 5.0 mm, while the total height of the system was balanced at 6.0 mm. All of the results and an ideal design are presented in the following section.

In proceeding with the calculations, a few geometric constraints were set for the wearable thermoelectric generator system. Since the system was planned to be worn much like a wristwatch, the device was constrained to a 2.0 cm wide and 21.0 cm long band that wrapped around the user's wrist and had an overall thickness of 1.0 cm. Aside from the geometric constraints, the properties of the materials used, such as the thermoelectric material and air, were chosen at the appropriate temperatures. Since the ambient temperature was assumed to be 300 K, the thermal properties of air at 300 K were used. The values used for air, along with all the other values used in this analysis, are summarized in Table 1.

3. Results and discussion

3.1. Heat dissipation

To begin, the heat sink's gap size and fin thickness were altered for a given fin height to minimize its thermal resistance—the cold side thermal resistance. In thermoelectric generation applications,

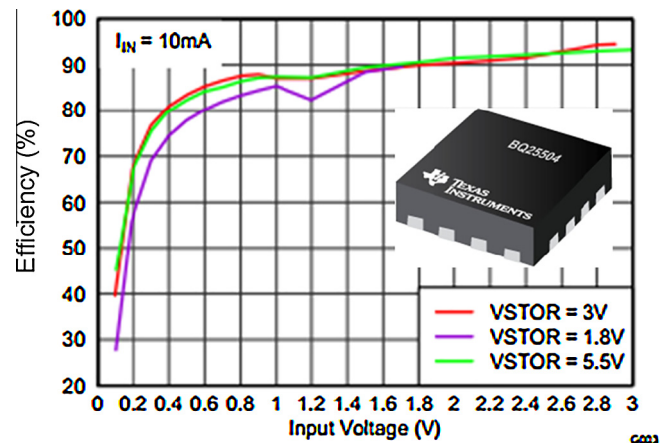


Fig. 3. The efficiency of the TI BQ25504 at different input voltages [22].

Table 1

The nomenclature and values used in the analysis.

Description	Variable	Units	Value
<i>Nomenclature</i>			
Thermoelectric material thermal conductivity	k	W/m K	1.820
Thermal conductivity of air	k_{air}	W/m K	0.0263
Thermoelectric material electrical resistivity	ρ	Ω m	7.226E-6
Leg cross-sectional area	A_C	m ²	Varied
Module surface area	A_S	m ²	4.200E-3
Number of thermoelectric leg pairs	N	1	100, 500, 1000
Thermal resistance (hot side)	ψ_H	m ² K/W	3.218
Thermal resistance (cold side)	ψ_C	m ² K/W	Calculated
Thermal resistance (thermoelectric module)	ψ_{TEM}	m ² K/W	Calculated
Thermoelectric figure of merit	ZT	1	Varied
Module Seebeck coefficient	S	V/K	Calculated
Seebeck coefficient of the p-type leg	α_p	V/K	9.000E-5
Seebeck coefficient of the n-type leg	α_n	V/K	9.000E-5
Module electrical resistance	R	Ω	Calculated
Average thickness of human skin	t_{skin}	m	0.005
Thermal conductivity of human skin	k_{skin}	W/m K	0.370
Contact area between the thermoelectric generator and users wrist	A_{skin}	m ²	4.200E-3
Number of heat sink fins	n	1	Calculated
Convective heat transfer coefficient	h	W/m ² K	Calculated
Perimeter of a single fin	P	m	Calculated
Fin cross-sectional	A_{fin}	m ²	Calculated
Thermal conductivity of heat sink material (aluminum)	k_{sink}	W/m K	237
Nusselt number for right-side up fin array	\overline{Nu}_D	1	Calculated
Nusselt number for upside down fin array	\overline{Nu}_t	1	Calculated
Nusselt number for a horizontal infinite flat plate	\overline{Nu}_l^2	1	Calculated
Rayleigh number for right-side up fin array	Ra_D	1	Calculated
Rayleigh number for upside down fin array	Ra_t	1	Calculated
Gravitational acceleration	g	m/s ²	9.810
Width of channel	D	m	Varied
Fin height	H	m	0.001–0.005
Volumetric thermal expansion coefficient of air	β	1/K	3.430E-3
Thermal diffusivity of air	κ	m ² /s	2.250E-5
Kinetic viscosity of air	ν	m ² /s	1.589E-5
Heat passing through the hot side	Q_H	W	Calculated
Heat passing through the cold side	Q_C	W	Calculated
Thermal conductivity of the module	K	W/K	Calculated
Electrical current	I	A	Calculated
Temperature (hot side)	T_H	K	Calculated
Temperature (cold side)	T_C	K	Calculated
Temperature (body)	T_{BODY}	K	310
Ambient temperature	T_∞	K	293
Fin array half-length	L	m	0.105

the cold side's thermal resistance is often much greater than the hot side's and must be decreased, as a high cold side thermal resistance reduces the maximum power generation of the thermoelectric generator. To evaluate the thermal resistance of the heat sink, the previously presented Nusselt number correlations for a right-side up heat sink were used. In calculating the Rayleigh number, the temperature difference between the heat sink and the ambient was assumed to be 5 K. Also, a lower limit of 1 mm was set for the fin thickness in order to take into account structurally practical fin thicknesses. Fig. 4 shows how the heat sink's thermal resistance varies with the gap size and fin thickness for a fin height of 4.0 mm.

As shown in Fig. 4, the heat sink's thermal resistance relied more on the gap size than the fin thickness. This is shown by the intense fluctuation in the thermal resistance when the gap size was altered. Also, when the fin thickness was as small as structural practicality allowed, the heat sink's thermal resistance reached a local minimum. Typically, the cross-sectional area of fins on a heat sink undergoing natural convection should be large enough to allow for heat to easily conduct through the entire length of the fin. However, the height of the fins was only 4.0 mm, which was not tall enough for the fin thickness to affect the conduction through the fins. Therefore, decreasing the fin thickness allowed for more fins on the heat sink, which provided a greater surface area for the heat sink and allowed for more heat transfer from the heat sink. With this information, better designs for heat sinks

used in wearable thermoelectric generators can be gained by simply allowing for more fins on the heat sink when the fin height is relatively short.

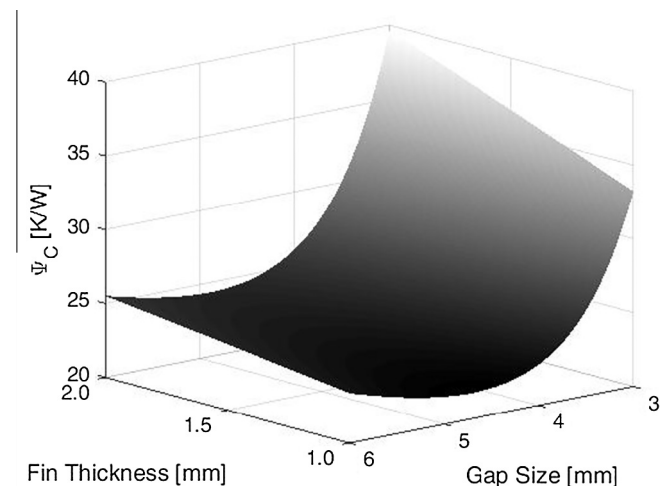


Fig. 4. The heat sink's thermal resistance versus a range of gap sizes and fin thicknesses for a fin height of 4.0 mm (the minimum thermal resistance is 21.7433 K/W).

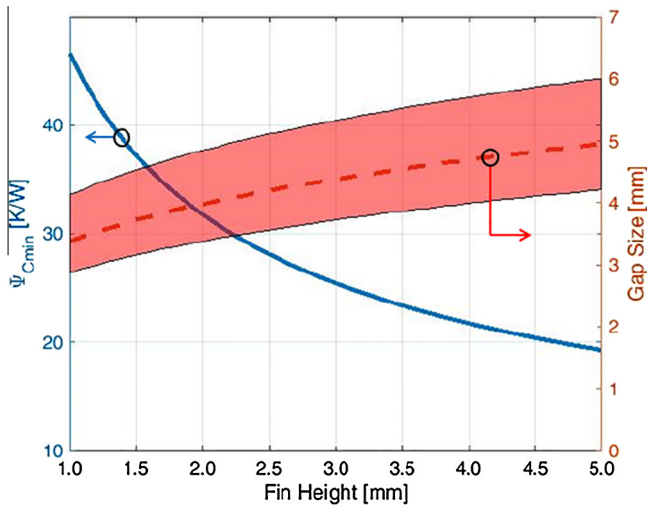


Fig. 5. The minimum cold side thermal resistance and the corresponding gap size versus the fin height. The shaded gap sizes allow for a thermal resistance within 5% of the minimum value. The fin thickness was given a constant value of 1.0 mm.

In seeing how the minimum heat sink thermal resistance varied with the gap size and fin thickness, the fin height was altered with a constant fin thickness of 1.0 mm to see the variation of the thermal resistance. Fig. 5 shows the minimum cold side thermal resistance with respect to the fin height, as well as the corresponding gap sizes and those that yield within 5% of the minimum thermal resistance for a given fin height.

As seen in Fig. 5, the minimum thermal resistance for an optimized heat sink decreased and the corresponding gap size increased as the fin height increased. Also, as seen in Fig. 5, the cold side thermal resistance was rather sensitive to the fin height, but not as sensitive to the gap size. This supports the idea that the fin height was the dominant geometric parameter of the heat sink, as it altered the thermal resistance of the heat sink more than the fin thickness or gap size. With this knowledge, the fin height should be altered first when optimizing a heat sink and the fin thickness and gap size should be altered after to add slight changes to the thermal resistance of the heat sink.

After analyzing the heat sink's thermal resistance through its geometric aspects, the thermoelectric generator was analyzed with consideration of a boost converter. Specifically, the module geometry was analyzed with respect to the thermal resistance of the heat sink to see how the heat sink's thermal resistance influenced the optimal module geometry. The parameter of concern in this analysis was the output power of the generator, as it varied based on both the thermal resistance of the heat sink and the module geometry. In drawing conclusions about the module geometry with respect to the maximum power generation, the B-factor was used. To begin the analysis, the temperatures on the hot and cold sides of the generator were found for multiple combinations of B-factors and heat sink thermal resistances using Eqs. (15) and (16). After, the power generation for each combination was calculated using Eq. (25), which was derived by Gomez et al. [7]. The B-factors that allowed for the maximum power generation at a specified thermal resistance were deemed the optimum B-factors.

In finding the optimum B-factors, it was noticed that their values were too large for practical purposes in wearable thermoelectric power generation, as the optimum B-factors were much higher than the B-factors of commercially sold modules. According to Eq. (13), a high B-factor meant the fill factor was low compared to the thermoelectric leg length. Since thermoelectric leg lengths are typically on the order of millimeters, it was implied that the

cross-sectional area of the thermoelectric legs was very small (less than 0.25 mm^2). Because of this, obtaining the optimum B-factor was thought to be impossible for a wearable thermoelectric power generator due to mechanical instability. Therefore, module geometries with a fill factor greater than 5% or a leg cross-sectional area of at least 0.25 mm^2 were considered along with the optimal B-factors in this analysis. In the practical case, the greatest B-factor was thought to provide the greatest power output for the generator. Fig. 6 shows the practical and optimum B-factors, which allowed for the maximum power outputs in each case, for a specified cold side thermal resistance with consideration of a boost converter. The B-factor range for which 95% of the maximum power output was generated is also shown for specific heat sink thermal resistance. Additionally, the previously presented Nusselt number correlations were used to calculate the thermal resistance values for an optimized heat sink with 4.0 mm tall fins facing entirely upward and downward. In plotting these values in Fig. 6, a conservative range in which the cold side thermal resistance fell was created, as the thermoelectric generator wrapped around a person's wrist, and therefore, had parts of its heat sink facing upward, downwards, and sideways. Using the thermal resistance range, a range of optimal B-factors that allowed for 95% of the maximum power output, no matter the orientation of the heat sink, was created, as shown by the green box in Fig. 6. In Fig. 7, the maximum power outputs associated with the optimum and greatest practical B-factors are displayed.

As seen in Fig. 6, the optimum B-factors are much greater than the practical B-factors, showing the difficulty in creating a wearable thermoelectric generator using the optimum B-factor. In considering practicality, the largest B-factor allowed for the maximum power generation; however, in ignoring practicality, the largest B-factor did not necessarily allow for the maximum power generation. The thermal resistance values for the optimized heat sink facing upward and downward, as shown in Fig. 6, were found to be 21.74 K/W and 53.35 K/W, respectively. With these values, the range of optimum B-factors—encompassed by the green box—that allowed for at least 95% of the maximum power output, regardless of the heat sink's orientation, was found. In addition, Fig. 7 shows

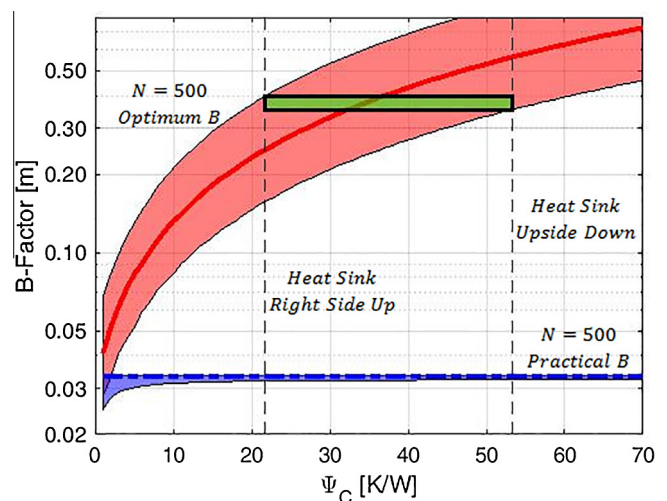


Fig. 6. The optimum and greatest practical B-factors versus the cold side thermal resistance for a theoretical generator of 500 leg pairs. The shaded region represents all B-factors that allow for 95% of the maximum power generation in the corresponding case. The green box shows a range of optimum B-factors that allow for 95% of the maximum power output, no matter the orientation of the heat sink (the maximum practical B-factor is 0.0336 m). (For interpretation of the references to colour in this figure legend, the reader is referred to the web version of this article.)

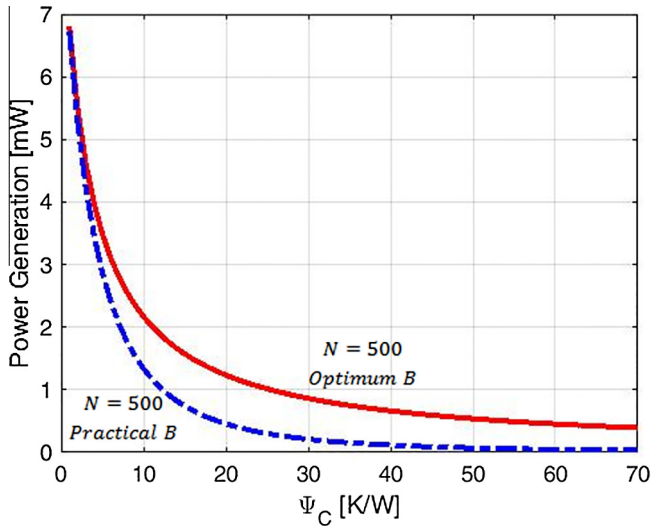


Fig. 7. The maximum power generation of theoretical generators of 500 leg pairs with the optimum and greatest practical B-factors versus the cold side thermal resistance.

the power generation for the optimum and greatest practical B-factors. Depending on the thermal resistance of the heat sink, the difference in power generation from the optimum B-factor could be substantial. In understanding these results for practical purposes, thermoelectric generators should be designed to have the highest B-factor possible while retaining structural stability within the module.

A final module aspect that was considered was the number of thermoelectric leg pairs. As inferred by the absence of the number of leg pairs in Eqs. (15) and (16), utilizing the B-factor provides an optimization process independent of the number of leg pairs when a boost converter is not considered. However, when a boost converter is implemented into the system, the number leg pairs has an effect on the system's performance. This is because the efficiency of a boost converter relies heavily on its input voltage, otherwise recognized as the module's output voltage. Since a module's output voltage relies on the number of leg pairs in a module, it is understood that the power generation and voltage output of a generator system are affected by the number of leg pairs in the

module. Fig. 8 shows how the maximum power generation and corresponding B-factor changed with the number of leg pairs for the optimum and practical cases when considering the implementation of a boost converter in the system. In creating this figure, the cold side thermal resistance was fixed at 21.7 K/W, the thermal resistance found earlier for an optimized heat sink facing upward.

As seen in Fig. 8, the maximum power generation for the optimum case was much larger than that of the practical case. However, the B-factors necessary for the optimum case were also much larger than practicality could support. It is seen that there was no power generation for lower numbers of leg pairs in the practical case. This is because when the thermoelectric generator had fewer legs, it produced only a small voltage, which greatly reduced the efficiency of the boost converter. It is also seen that the peak maximum power generation for the practical case was 0.442 mW and occurred when there were 420 leg pairs in the module. This peak occurred because at 420 leg pairs, the thermoelectric power generator had a fill factor of 5% and a leg cross-sectional area of 0.25 mm². These aspects were previously set limitations for the structural stability of the thermoelectric generator. However, if further research is completed for improving the figure of merit of the thermoelectric material used in the generator, structural stability will no longer limit the maximum power generation of a wearable thermoelectric generator.

In general, altering the thermoelectric material properties to increase the thermoelectric figure of merit is a popular research area for thermoelectrics [2,3,15]. As shown by Eq. (8), increasing the figure of merit can be done by altering the following thermoelectric material properties in the indicated manner: increasing the Seebeck coefficient, decreasing the electrical resistivity, and decreasing the thermal conductivity. For wearable thermoelectric power generation, an increased figure of merit has the potential to allow for more power generation from thermoelectric generators of a similar B-factor. In this analysis, thermoelectric material properties were independently altered to double the figure of merit of a thermoelectric generator with 500 leg pairs and a B-factor of 0.0336 m. This allowed for the resulting power outputs from each material property alteration to be compared, providing a better sense of which thermoelectric material property contributes the most to the generated power of a wearable thermoelectric power generator. Table 2 shows the maximum power generation with

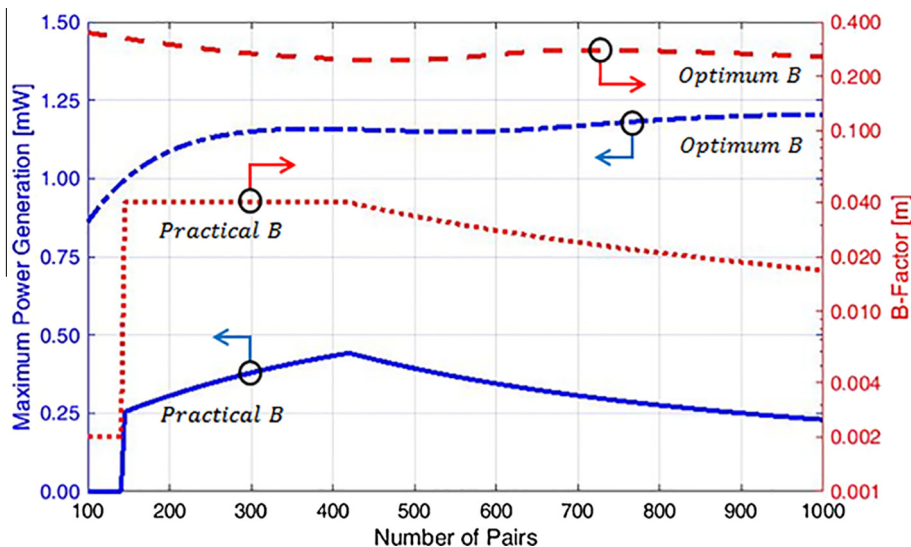


Fig. 8. The maximum power generations and the corresponding B-factors for the optimum and practical cases versus a varying number of leg pairs with consideration of a boost converter. The cold side thermal resistance was fixed at 21.7 K/W, the thermal resistance previously found for an optimized heat sink (maximum practical power generation = 0.442 mW at 420 leg pairs).

Table 2

The material properties used to double the figure of merit and the resulting maximum power generation.

Seebeck coefficient (V/K)	Thermal conductivity (W/m K)	Electrical resistivity (Ω m)	ZT	Max. power generation (W)
<i>Improving the figure-of-merit</i>				
1.80E-04	1.82	7.23E-06	0.74	1.09E-03
2.54E-04	1.82	7.23E-06	1.47	1.89E-03
1.80E-04	0.91	7.23E-06	1.47	1.52E-03
1.80E-04	1.82	3.61E-06	1.47	1.83E-03

the corresponding thermoelectric material properties. The first row in Table 2 provides a reference for observing the effects of doubling the figure of merit by altering each property.

As shown in Table 2, any improvements to the thermoelectric material properties allowed for a substantial increase in the maximum power generation of the thermoelectric generator. However, doubling the figure of merit by increasing the Seebeck coefficient allowed for the largest increase in the maximum power generation, closely followed by reducing the electrical resistivity. In seeing the effects of doubling the figure of merit to the maximum power generation of the system, the importance of research in improving thermoelectric material properties can be seen.

3.2. Power conditioning/boost converter

Since the total power and voltage outputs were the main concerns in creating the wearable thermoelectric generator, it was important to know how these values were affected when a boost converter was implemented into the system. In gaining this knowledge, a thermoelectric power generator can be modified to gain the maximum power output from the system. Using Eq. (25), the theoretical maximum power generation for a thermoelectric generator using modules with the greatest practical B-factor was found with and without consideration of a boost converter. To do this, the electrical loading resistance ratio was varied until a maximum power generation was found. Fig. 9 shows the maximum output powers for the thermoelectric generator with and without consideration of a boost converter (TI BQ25504) for the greatest practical B-factor.

As shown in Fig. 9, when the greatest practical B-factor was considered for a generator of 500 leg pairs, the system produced 0.54 mW of power without consideration of a boost converter and 0.38 mW of power with consideration of a boost converter. Also, as seen in Fig. 9, the voltage at which the maximum power happens with consideration of the boost converter is not the same as the voltage for when the boost converter is not considered. This provides evidence that neither the traditional method nor the thermal load matching method can be used to obtain the maximum power generation, as the maximum output power depends on the voltage value. Therefore, if a boost converter is implemented into the system, the maximum output power from the generator may decrease, but the voltage at which the maximum happens will increase.

3.3. Physical size & aesthetics

Since wearing bulky objects is undesirable, realistic size constraints for the thermoelectric generator were considered. As previously demonstrated, limiting the system's geometric parameters makes optimization necessary to minimize the thermal resistance of the cold side of the device and obtain a high performing thermoelectric generator. In this analysis, the overall allowed thickness of the system (10.0 mm) was portioned between the fin height and the thermoelectric leg length in a multitude of ratios to find an optimum ratio. Since the contact pads used in the device

were assumed to be a maximum of 4.0 mm thick, the total thickness available for the fin height and leg length was 6.0 mm. To analyze the geometric aspects, the maximum output power was determined for many combinations of fin heights and leg lengths, where the fin heights ranged from 1.0 mm to 5.0 mm with the corresponding leg lengths. Fig. 10 shows the maximum output power versus the heat sink fin height, paired with the thermoelectric leg length. The B-factors that allowed for 90% or more of the maximum output power are also plotted against the same length values. In gaining the data, a fin thickness of 1.0 mm and a gap size of 4.7 mm were used with a theoretical generator of 500 leg pairs.

As shown in Fig. 10, the theoretical maximum output power of the system, which assumes the device is fully in contact with the wrist and the optimal load matching condition is achieved, was found to increase with the fin height. This implies that the fin height is the dominant geometric aspect over the module leg length for obtaining the maximum power generation from the system when the B-factor is limited by practicality. Also shown in the figure, the range of B-factors that allow for 90% or more of the maximum power obtained for a specific fin height slightly increases with the fin height. In seeing that the fin height is the dominant geometric aspect when practicality is considered, the generator should be designed such that there is a high ratio of fin height to leg length. Considering the following practical geometric parameters, a maximum power generation of 0.48 mW can be obtained by the generator system: module leg length of 1.0 mm, fin height of 5.0 mm, fin thickness of 1.0 mm, gap size of 4.7 mm, 500 legs, and a B-factor of 0.336 m.

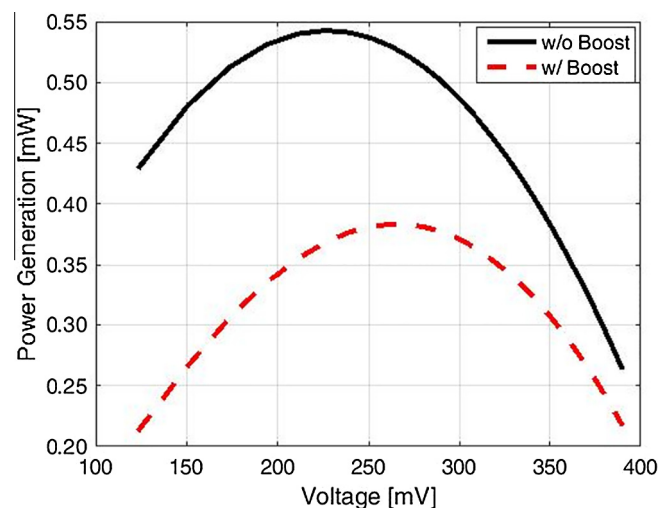


Fig. 9. The output power versus the output voltage of a wearable thermoelectric generator with and without consideration of the boost converter. The generator used had a B-factor of 0.0336 m with 500 leg pairs and the heat sink was assumed to be optimized with a fin height of 4.0 mm ($\psi_c = 22.0$ K/W) (the maximum power generation without the boost converter is at $P = 0.54$ mW and $V = 226.3$ mV) (the maximum power generation with the boost converter is at $P = 0.38$ mW and $V = 262.2$ mV).

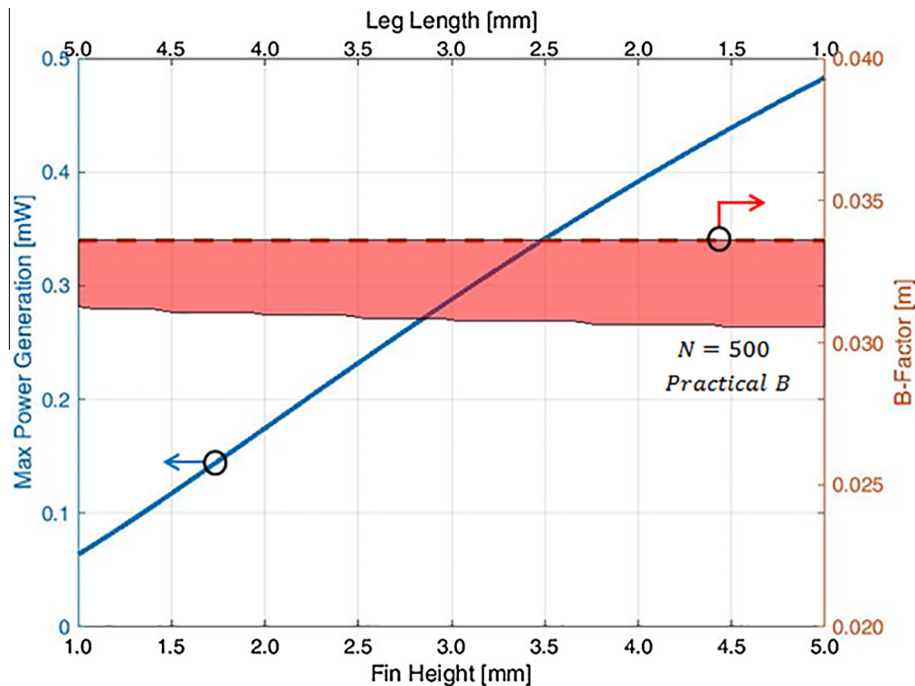


Fig. 10. The maximum output power of the system and B-factor plotted against the heat sink fin height and thermoelectric leg length (fin thickness = 1.0 mm, Gap size = 4.7 mm, $N = 500$).

In addition to the projected outputs, a mock-up of the wearable thermoelectric generator is proposed as shown in Fig. 11. Modeled after a traditional watch band design, the proposed device employs small modules that have heat sinks on their cold sides. These modules are linked together side-by-side with a pin, which allows for a large range of movement and rotation. Linking the modules in this way also assists the modules in making contact with the user's skin all the way around the user's wrist. Additionally, the pin contains an electrically conductive portion that is insulated from the environment and allows for the modules to be connected electrically in series. Designing the wristband in this way will allow for a purposeful thermoelectric heat generator to be created.

In order to improve upon this design, incorporating flexible thermoelectric modules could allow for better contact between the modules and the user's skin [15,16]. With further research in flexible thermoelectrics, vast enhancements to wearable thermo-

electric power generators could be made and new products can be developed.

4. Conclusions

In designing an effective wearable thermoelectric generator, three practical issues of system integration must be considered: the limited heat dissipation from the cold side of the module, the low voltage reality of thermoelectric devices, and the overall size of the wearable device. Since a boost converter was used to increase the output voltage of the system, neither the traditional method nor the thermal load matching method could be used to optimize the generator. Furthermore, it was found that with the current materials and boost converters, practicality in design disallowed the optimum B-factor from being used, prohibiting the system from performing at its full potential and gaining its maximum power output. In designing the heat sink for the generator, the fin height was the dominating factor for reducing the generator's cold size thermal resistance and providing the greatest output power. After optimizing a heat sink for natural convection and the module geometry within the practical constraints, a potential output of 0.48 mW at 3.0 V produced purely by body heat was calculated with the consideration of a boost converter for a thermoelectric generator with a total area of 42 cm² and a total thickness of 1.0 cm. Due to its high output voltage, the thermoelectric generator was determined to be capable of powering small electrical devices. With known theoretical values, this paper calls for an experimental effort to build a prototype of a single link to provide experimental validation for the modeling results.

Acknowledgements

We would like to acknowledge the School of Engineering at Santa Clara University and the Kuehler Grant for their financial

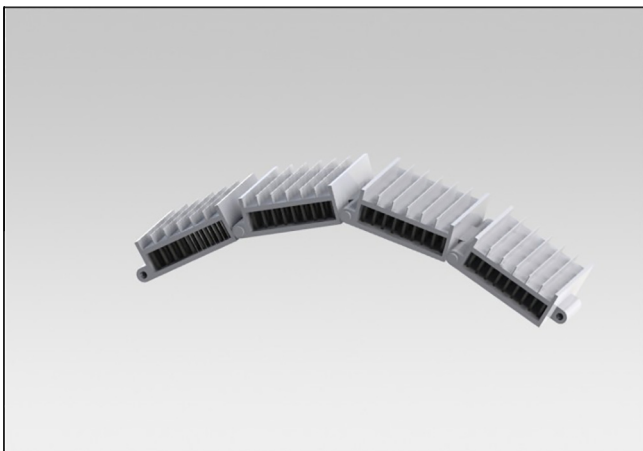


Fig. 11. A sample of the thermoelectric generator wristband links, including the thermoelectric modules and attached heat sinks.

support. We would also like to thank Joseph Singer and Thomas Watson for assisting in the editing of our manuscript.

References

- [1] McCarty R. Thermoelectric power generator design for maximum power: it's all about ZT. *J Electron Mater* 2012;42.
- [2] Poudel B, Hao Q, Ma Y, Lan Y, Minnich A, Yu B, et al. High-thermoelectric performance of nanostructured bismuth antimony telluride bulk alloys. *Science* 2008;320:634–8.
- [3] Tang X, Xie W, Han L, Wenyu Z, Qingjie Z, Niino M. Preparation and thermoelectric transport properties of high-performance Bi₂Te₃ with layered nanostructure. *Appl Phys Lett* 2007;90:012102–012102-3.
- [4] Rowe MD. *CRC handbook of thermoelectrics*. CRC Press; 1995.
- [5] Angrist SW. *Direct energy conversion*. 4th ed. Allyn and Bacon, Inc.; 1982.
- [6] Gomez M, Reid R, Ohara B, Lee H. Influence of electrical current variance and thermal resistances on optimum working conditions and geometry for thermoelectric energy harvesting. *J Appl Phys* 2013;113:174908-1–8-8.
- [7] Gomez M, Ohara B, Reid R, Lee H. Investigation of the effect of electrical current variance on thermoelectric energy harvesting. *J Electron Mater* 2013;1–8.
- [8] Yazawa K, Shakouri A. Optimization of power and efficiency of thermoelectric devices with asymmetric thermal contacts. *J Appl Phys* 2012;111.
- [9] Youn N, Lee H, Wee D, Gomez M, Reid R, Ohara B. Achieving maximum power in thermoelectric generation with simple power electronics. *J Electron Mater* 2014;43:1597–602.
- [10] McCarty R, Piper R. Voltage-current curves to characterize thermoelectric generators. *J Electron Mater* 2015;44:1896–901.
- [11] Leonov V, Torfs T, Fiorini P, Van Hoof C. Thermoelectric converters of human warmth for self-powered wireless sensor nodes. *IEEE Sensors J* 2007;7:650–7.
- [12] Leonov V, Vullers RJM. Wearable thermoelectric generators for body-powered devices. *J Electron Mater* 2009;38:1491–8.
- [13] Suarez F, Nozariasbmarz A, Vashaee D, Ozturk M. Designing thermoelectric generators for self-powered wearable electronics. *Energy Environ Sci* 2016;9:2099–113.
- [14] Francioso L, De Pascali C, Farella I, Martucci C, Creti P, Siciliano P, et al. Flexible thermoelectric generator for ambient assisted living wearable biometric sensors. *J Power Sources* 2011;196:3239–43.
- [15] Chen Y, Zhao Y, Liang Z. Solution processed organic thermoelectrics: towards flexible thermoelectric modules. *Energy Environ Sci* 2015;8:401–22.
- [16] Bahk J, Fang H, Yazawa K, Shakouri A. Flexible thermoelectric materials and device optimization for wearable energy harvesting. *J Mater Chem C* 2015;3:10362–74.
- [17] Min-Ki K, Myoung-Soo K, Seok L, Chulki K, Yong-Jun K. Wearable thermoelectric generator for harvesting human body heat energy. *Smart Mater Struct* 2014;23:105002.
- [18] Wang Z, Leonov V, Fiorini P, Van Hoof C. Realization of a wearable miniaturized thermoelectric generator for human body applications. *Sens Actuat A* 2009;156:95–102.
- [19] Bergman TL, Lavine AS, Incropera FP, DeWitt DP. *Fundamentals of heat and mass transfer*. 7th ed.; 2011.
- [20] Bejan A. *Convection heat transfer*. 4th ed. Wiley; 2013.
- [21] Dayan A, Kushnir R, Mittelman G, Ullmann A. Laminar free convection underneath a downward facing hot fin array. *Int J Heat Mass Transf* 2003;47:2849–60.
- [22] BQ. Ultra low-power boost converter with battery management for energy harvester applications. Texas Instruments; June 2015. Web 28 May 2016. <<http://www.ti.com/lit/ds/symlink/bq25504.pdf>>.